

Chiral Symmetry and hadron properties at finite temperature – A numerical experiment

Teiji Kunihiro¹, Shin Muroya², Atsushi Nakamura^{3,4,5}, Chiho Nonaka^{6,7}, Motoo Sekiguchi⁸, Hiroaki Wada⁸, and Masayuki Wakayama^{3,5}

¹*Department of Physics, Kyoto University, Kyoto 606-8502, Japan*

²*Faculty of Comprehensive Management, Matsumoto University, Matsumoto 390-1295, Japan*

³*School of Biomedicine, Far Eastern Federal University, 690950 Vladivostok, Russia*

⁴*Research Center for Nuclear Physics (RCNP), Osaka University, Ibaraki, Osaka, 567-0047, Japan*

⁵*Theoretical Research Division, Nishina Center, RIKEN, Wako 351-0198, Japan*

⁶*Kobayashi Maskawa Institute, Nagoya University, Nagoya 464-8602, Japan*

⁷*Department of Physics, Nagoya University, Nagoya 464-8602, Japan*

⁸*School of Science and Engineering, Kokushikan University, Tokyo 154-8515, Japan*

.....
We study the hadron properties at finite temperature from measurement of the screening masses, using two-flavor full QCD of the hybrid Monte Carlo (HMC) algorithm with the renormalization group improved Iwasaki gauge action and the clover improved Wilson quark action on a $16^3 \times 4$ lattice. We explore rather heavy quark mass regions. Disconnected quark diagram is dropped. We observe the tendency that the screening masses in all the channels degenerate, which is in accord with the effective restoration of $U_A(1)$ symmetry, and then eventually approach $2\pi T$, i.e. the free quark value. In the low temperature region below pseudocritical temperature T_c , the screening masses in all the channels decrease. We discuss the different features between these calculations and the previous ones.
.....

Subject Index xxxx, xxx

1. Introduction

Hadrons are elementary excitations on top of the nonperturbative QCD (Quantum Chromodynamics) vacuum where (colored) free quarks and gluons do not exist in the asymptotic states. The properties are called color confinement. Furthermore, the QCD vacuum is characterized by the dynamical breaking of (approximate) chiral symmetry (DBCS) and $U_A(1)$ anomaly. The DBCS manifests itself as the appearance of the nearly massless pseudoscalar mesons with the peculiar coupling properties. On the other hand, the axial anomaly is, for instance, responsible for the large mass of $\eta'(958)$ compared with the other low-lying eight pseudoscalar mesons and the small mixing angle with $\eta(550)$ in the flavor $SU(3)_f$ basis. Moreover the axial anomaly can account for the large mass difference of the pion and the a_0 .

A unique feature of the QCD vacuum is that it should undergo a phase transition to chiral-symmetric phase at high temperature (T) and/or high baryon chemical potential. The axial anomaly may also be effectively restored in such an extreme condition [1]. Thus we can expect that hadrons

on top of the new ground state or thermal equilibrium state may change their properties along with that of the QCD vacuum [2–5]; in turn, (colorless) hadronic excitations with a small width may exist in the low-energy region even in the quark-gluon plasma (QGP) phase as the soft modes of the chiral transition [2, 3] and the hydrodynamic modes [6].

The restoration of chiral symmetry should lead to degeneracy of the hadron spectral functions in the channels of the chiral partners: in the chiral $SU(2)_L \times SU(2)_R$ symmetry, the chiral partner of the pion is the sigma meson (isoscalar-scalar) while that of the isovector-vector meson ρ is the isovector-axial vector meson a_1 . On the other hand, the pion and a_0 mesons are the partner in terms of $U_A(1)$ symmetry. Conversely speaking, the rate of the degeneracy of the spectral functions in the channels of the chiral partners can be used as a measure of the symmetry restoration.

The first calculation of the chiral partners in the scalar channels based on a chiral effective model [2–5] showed that the sigma meson becomes soft and tends to get degenerate with the pion near the pseudocritical temperature T_c of the chiral phase transition. QCD sum-rule calculations [7] showed that the masses of the ρ and its chiral partner a_1 both decrease at finite T , although their possible degeneracy toward the critical temperature is obscure depending on the calculation method.

In the present work, we explore the hadron properties at finite temperature using the lattice simulations of QCD. We study the screening masses [8, 9] obtained from the current-current correlations in the spatial direction. Indeed, some authors [10–12] performed lattice-QCD simulations of the static screening masses at finite temperature including the critical (crossover) temperature and tried to extract the strength of the $U_A(1)$ anomaly in the chiral limit as well as the behavior of the screening masses of the chiral partners in the scalar and vector channels: in Ref. [11] where the highly improved staggered quark (HISQ) action is used as in Ref. [10], it is shown that the screening masses of the positive parity mesons decrease whereas those of the negative parity mesons monotonically increase with temperature and thereby tend to get degenerate; they eventually approach $2\pi T$ above the critical temperature. This behavior is consistent with the chiral degeneracy and shows a possible scenario of the way how the chiral symmetry is restored in the vector and axial-vector channels. It is, however, to be noted that this scenario is quite different from that suggested in [7]; see also a recent analysis at finite density [13]. It is conceivable that the hadronic modes are modified by usual thermal effects as described by the hadron resonance gas model [14]; the intrinsic QCD dynamics becomes an essential ingredient for determining the properties of the hadronic modes just around the critical point. Thus it should be helpful for identifying the underlying mechanism of spectral changes of hadronic modes to explore the thermal behavior of the screening masses at finite T using different quark actions with various quark masses.

We dare to make simulations of the screening masses using rather heavy quark masses. In this way, the number of thermally excited hadrons are suppressed, and consequently, they would hardly contribute to the thermodynamics of the system. We expect that such a simulation of the extreme set up far away from the chiral limit may provide us with the basic ingredients to realize the spectral changes of hadrons obtained in more complete lattice simulations.

We find that below T_c , not only positive-parity screening masses but negative-parity screening masses also decrease in contrast to the findings given by the simulations respecting chiral symmetry [11, 12]. As for the effective restoration of $U_A(1)$ symmetry, for which the intrinsic dynamics of QCD is responsible, our simulation shows that it manifests itself as a drop of the positive-parity screening masses and an increase of the corresponding negative-parity screening masses above T_c and degenerate at very high temperature in accord with the previous simulations with different quark actions [11, 12].

The paper is organized as follows: in Sec. 2, we explain simulation parameters of our two-flavor full lattice QCD calculation. In Sec. 3, we show calculated results of screening masses of scalar, pseudoscalar, vector and axial-vector channels as a function of the gauge coupling β and the ratio of temperature to the pseudocritical temperature T/T_c . We also discuss quark mass dependence of them. Section 4 is devoted to summary and discussion.

2. Lattice simulations

We generate the gauge configurations in two-flavor full QCD using the hybrid Monte Carlo (HMC) algorithm with the renormalization group improved Iwasaki gauge action and the clover improved Wilson quark action on a $16^3 \times 4$ lattice. Here we investigate hadron properties at finite temperature with relatively heavy quark masses, hoping to identify the basic ingredients for realizing the temperature dependence of screening masses, using different gauge and fermion actions in lattice QCD. The pseudo-critical temperature T_c in the present work is determined from the peak position of the susceptibility of the Polyakov loop, which is supposed to describe the confinement-deconfinement transition modified by the presence of quarks even if their masses are heavy. We use the same combinations of the gauge couplings β and hopping parameters κ as those in Ref. [15] in which they also evaluate the corresponding temperature. The coefficient c_{SW} in the clover improved Wilson quark action is given by $c_{SW} = (1 - 0.8412\beta^{-1})^{-3/4}$ [15]. The simulation parameters are listed in Table 1. In the case of $m_{ps}/m_v = 0.75$ values of ratio T/T_c do not contain errors, because we read off values of κ and β along the $m_{ps}/m_v = 0.75$ line from Fig. 1 in Ref. [15]. We update the first 1500 trajectories in the quenched QCD and switch to a simulation with the dynamical fermion. We discard the next 2000 trajectories of HMC and start to save the gauge configurations every ten trajectories.

Table 1 Simulation parameters for $m_{ps}/m_v = 0.65, 0.75$ and 0.80 [15]. We produce 1000 gauge configurations for each parameter.

$m_{ps}/m_v = 0.65$			$m_{ps}/m_v = 0.80$		
β	κ	T/T_c	β	κ	T/T_c
1.90	0.141849	1.32(5)	1.60	0.143749	0.80(4)
2.00	0.139411	1.67(6)	1.70	0.142871	0.84(4)
$m_{ps}/m_v = 0.75$			1.80	0.141139	0.93(5)
β	κ	T/T_c	1.85	0.140070	0.99(5)
1.55	0.146479	0.80	1.90	0.138817	1.08(5)
1.96	0.138732	1.35	1.95	0.137716	1.20(6)
2.06	0.137254	1.70	2.00	0.136931	1.35(7)
			2.10	0.135860	1.69(8)
			2.20	0.135010	2.07(10)
			2.30	0.134194	2.51(13)
			2.40	0.133395	3.01(15)

Assuming that mesons are composed of two quarks, we employ simple point-like sources and sinks for the construction of meson operators,

$$M(x) = \sum_{c=1}^3 \sum_{\alpha,\beta=1}^4 \bar{q}_\alpha^c(x) \Gamma_{\alpha\beta} q_\beta^c(x), \quad (1)$$

where $q(x)$ is the Dirac operator for the u/d quark and $\Gamma_{\alpha\beta}$'s stand for I , γ_5 , γ_μ and $\gamma_\mu\gamma_5$ for the scalar, the pseudoscalar, the vector and the axial-vector channels. The indices c and α are the color and Dirac-spinor indices, respectively. Here we measure spatial correlation functions of mesons in the z direction. The spatial correlation function of the scalar channel is composed of connected and disconnected diagrams. In order to calculate the disconnected diagram, we employ the Z_2 noise method and subtract the vacuum expectation value of them [16].

3. Calculated results

In Fig. 1 we show screening masses of the pseudoscalar, the scalar, the vector and the axial-vector channels as a function of the gauge coupling β and T/T_c . The statistical errors are estimated by the jackknife method with the bin size of 10. We extract the screening masses from exponential damping of the spatial correlation functions in $3 < z < 15$. In the scalar channel, we obtain the connected part of the spatial correlation with small errors; however, we confront severe noise in the calculation of the disconnected part even on the 1000 gauge configurations. Therefore, in this paper, we evaluate the screening masses of the scalar channel by using only the connected part. In the two-flavor QCD the connected part of the scalar channel can be regarded as the a_0 meson. In the low temperature

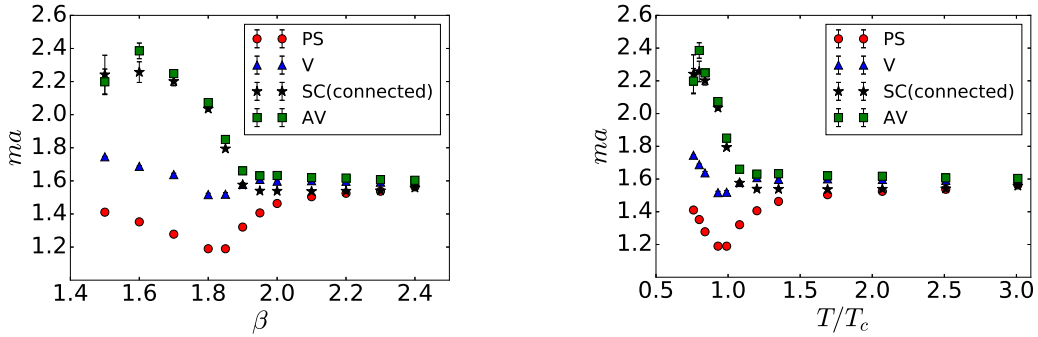


Fig. 1 The screening masses as a function of the gauge coupling β (left) and the ratio of temperature to the pseudocritical temperature T/T_c (right), in the case of $m_{ps}/m_v = 0.80$. The red solid circles, the blue solid triangles, the black solid stars and the green solid squares denote the pseudoscalar (PS), the vector (V), the connected part of the scalar (SC), the axial-vector (AV) channels, respectively.

region below the pseudocritical temperature ($T/T_c < 1.0$), the screening masses in all the channels decrease with the gauge coupling β or the ratio T/T_c , except for the positive-parity hadrons at quite low temperature region. In particular, the screening masses of the scalar meson are heavier than

those of the vector meson and almost the same as the ones of the axial-vector meson. This result is consistent with the fact that the a_0 meson mass is heavier than the ρ meson mass. If we could include the disconnected diagram as well as the connected diagram in evaluation of screening masses in the scalar channel, we would obtain lower screening masses which are almost the same as those in the vector channel [16]. It is noteworthy that a simulation at almost physical quark mass on the gauge configurations generated in the (2+1)-flavor QCD with the HISQ action [10, 11] shows an increase of the screening masses in the negative parity channels, i.e. the pseudoscalar and vector channels along with increasing temperature in the low temperature region. Since the hadron resonances are not expected to contribute to the dynamics in our simulation with heavy quarks, the decrease might be mainly attributed to mutual interactions of hadron resonances but not to the possible change of the QCD vacuum.

Around the pseudocritical temperature T_c , the screening masses of negative parity mesons take a minimum value and above it they turn to increase with temperature. On the other hand, the screening masses of positive parity mesons, the scalar and axial-vector channels keep decreasing with temperature. Then around $\beta = 1.95$ ($T/T_c = 1.20$), the screening masses of negative parity mesons and positive parity mesons approach each other and degenerate at $\beta = 2.3$ ($T/T_c = 2.5$), i.e. much the same behavior as those found in Refs. [10, 11]. The degeneracy of the screening masses between the vector and the axial-vector channels suggests that the chiral symmetry is realized in this high temperature region although the symmetry is badly broken with heavy quark mass in the present simulation. As for the scalar and pseudoscalar channels, it is noteworthy that the degeneracy in the scalar and pseudoscalar channels is realized in spite of lack of the disconnected diagram in the scalar channel. Again this behavior implies that the chiral symmetry gets realized in the high temperature region in spite of the large current quark mass. Furthermore, the $U_A(1)$ anomaly is a key issue to understand relations between the pseudoscalar and scalar channels at finite temperature. In fact, in Ref. [12] they tried to extract the strength of the $U_A(1)$ anomaly from the mass gap of screening masses between the pseudoscalar and scalar channels in the chiral limit. However, because our current calculation is performed with relatively heavy quark, small lattice size and neglecting the disconnected diagram in the scalar channel we do not go further in the discussion on it.

At the highest temperature $\beta = 2.4$ ($T/T_c = 3.0$) we find that the screening masses in all the channels tend to get degenerate and approach $2\pi T$.

In Fig. 2 we show the screening masses of the pseudoscalar, the vector, the scalar from the connected diagram and the axial-vector channels as a function of T/T_c in the case of $m_{ps}/m_v = 0.65, 0.75$ and 0.80 . For $m_{ps}/m_v = 0.75$ ($m_{ps}/m_v = 0.65$), we evaluate the screening masses in each channel at $T/T_c = 0.80, 1.35$ and 1.70 ($T/T_c = 1.32$ and 1.67). For the axial-vector channel, due to the large errors in spacial correlation functions we fail to evaluate the screening mass at $T/T_c = 0.80$ in the case of $m_{ps}/m_v = 0.75$. We observe the tendency that the screening masses of all channels decrease with the ratio m_{ps}/m_v . In particular, we find a distinct drop of the screening mass in the pseudoscalar channel as the ratio m_{ps}/m_v becomes smaller. On the other hand, in the vector channel we observe relatively weak dependence on m_{ps}/m_v .

Figure 3 shows the screening masses in the pseudoscalar, the vector and the scalar channels from the connected diagram and the axial-vector channels as a function of the ratio m_{ps}/m_v , at $T/T_c = 1.69$ (top), $T/T_c = 1.35$ (bottom left) and $T/T_c = 0.80$ (bottom right). At first, the screening masses in all the channels become smaller with lighter quark masses, but the decreasing rate of them is different in each channel. In the case of $T/T_c = 1.69$, at the $m_{ps}/m_v = 0.80$ the complete degeneracy between the vector and the axial-vector channels is found; however, it tends to resolve as the quark

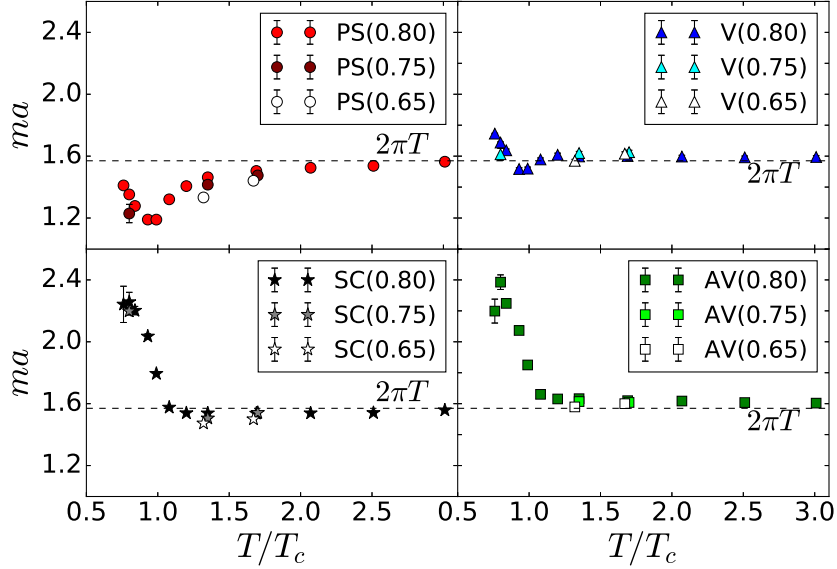


Fig. 2 The screening masses of the pseudoscalar (PS) (top left), the vector (V) (top right), the connected part of the scalar (SC) (bottom left) and the axial-vector (AV) (bottom right) channels as a function of T/T_c in the case of $m_{ps}/m_v = 0.65, 0.75$ and 0.80 . The dotted lines stand for $2\pi T$.

mass becomes smaller. We can see weaker trend to degeneracy between the pseudoscalar and the connected part of the scalar channels at $m_{ps}/m_v = 0.80$, but it also disappears at lighter quark masses. At $T/T_c = 1.35$ the difference of screening masses between the pseudoscalar and the vector channels is larger than that at $T/T_c = 1.69$. To obtain a rough idea of the value of screening mass of each channel at the physical quark mass, we draw the linear line which is obtained by fitting screening masses at $m_{ps}/m_v = 0.65, 0.75$ and 0.80 . The thick solid line represents the value of the physical quark mass. Because our quark masses are far from the physical value, the extrapolation should not be taken to be serious. However, it suggests that the clear degeneracy observed in our calculation might be a behavior specific to heavy quarks.

4. Summary and discussion

We have explored the hadron properties at finite temperature using two-flavor full QCD of the hybrid Monte Carlo (HMC) algorithm with the renormalization group improved Iwasaki gauge action and the clover improved Wilson quark action on a $16^3 \times 4$ lattice. In spite of the limited calculations with heavy quark mass, $m_{ps}/m_v = 0.80$, we have observed that at $T/T_c = 2.5$ the clear degeneracy between the screening masses of the negative parity mesons and the positive parity mesons. At the highest temperature $\beta = 2.4$ ($T/T_c = 3.0$) we find the tendency that the screening masses in all the channels degenerate in accord with the effective restoration of $U_A(1)$ symmetry, and then eventually approach $2\pi T$, namely, the free-quark value.

In the low temperature region below pseudocritical temperature T_c , the screening masses in all the channels decrease along with temperature, which is a different behavior from that found in the

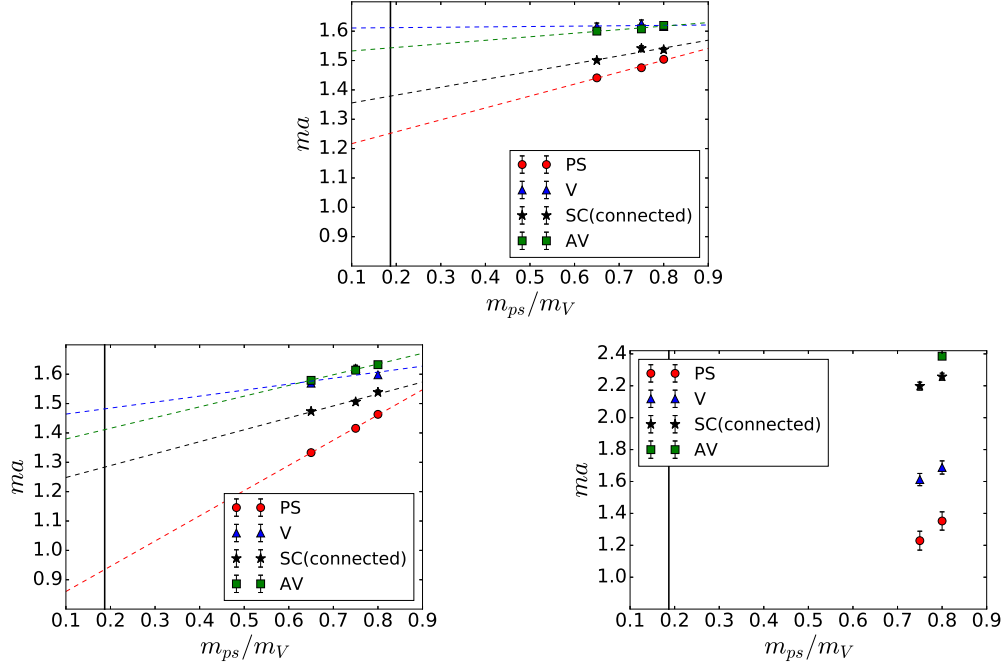


Fig. 3 The screening masses of the pseudoscalar (PS), the vector (V), the connected part of the scalar (SC) and the axial-vector (AV) channels as a function of the ratio m_{ps}/m_V in the case of $T/T_c = 1.69$ (top), $T/T_c = 1.35$ (bottom left) and $T/T_c = 0.80$ (bottom right), respectively.

previous calculation obtained at almost physical quark mass on the gauge configurations generated in the (2+1)-flavor QCD with the HISQ action [10, 11]. Our finding of the behavior of the screening masses may be a characteristic feature in the heavy quark sector because hadron gas resonance dynamics would not play any significant role in contrast to the simulations respecting chiral symmetry [10, 11]. Furthermore, we make a comment on a fermion lattice action. Here we utilized the clover improved Wilson quark action in which the chiral symmetry is explicitly broken. To elucidate physics related with the chiral symmetry, chiral fermion actions such as domain wall fermions and overlap fermions would be more suitable.

We have also investigated the quark mass dependence of behavior of the screening masses at finite temperature. The degeneracy which we find at high temperature above T_c between screening masses of the negative parity mesons and the positive parity mesons is resolved at lighter quark masses. To reach a conclusive result, we need to check the detailed behavior of screening masses of each channel such as lattice size and quark mass dependence of them.

Acknowledgment

The work of C.N. is supported by the JSPS Grant-in-Aid for Scientific Research (S) No. 26220707 and the JSPS Grant-in-Aid for Scientific Research (C) No. 17K05438. The work of T.K. and A.N. is partially supported by the JSPS Grant-in-Aid for Scientific Research (B) No. 15H03663. The work of S. M. is partially supported by the Grant-in-Aid of Matsumoto University for the Academic Research. The simulation was performed on an NEC SX-9 and SX-ACE supercomputers at RCNP,

Osaka University, and was conducted with the Fujitsu PRIMEHPC FX10 System (Oakleaf-FX, Oakbridge-FX) in the Information Technology Center, the University of Tokyo.

References

- [1] Robert D. Pisarski and Frank Wilczek, *Phys. Rev.*, **D29**, 338–341 (1984).
- [2] T. Hatsuda and T. Kunihiro, *Phys. Lett.*, **B145**, 7–10 (1984).
- [3] T. Hatsuda and T. Kunihiro, *Phys. Rev. Lett.*, **55**, 158–161 (1985).
- [4] T. Hatsuda and T. Kunihiro, *Prog. Theor. Phys.*, **74**, 765 (1985).
- [5] T. Hatsuda and T. Kunihiro, *Phys. Lett.*, **B185**, 304 (1987).
- [6] Carleton E. Detar, *Phys. Rev.*, **D32**, 276 (1985).
- [7] Tetsuo Hatsuda, Yuji Koike, and Su-Houng Lee, *Nucl. Phys.*, **B394**, 221–266 (1993).
- [8] Carleton E. Detar and John B. Kogut, *Phys. Rev. Lett.*, **59**, 399 (1987).
- [9] Carleton E. Detar and John B. Kogut, *Phys. Rev.*, **D36**, 2828 (1987).
- [10] Alexei Bazavov, Frithjof Karsch, Yu Maezawa, Swagato Mukherjee, and Peter Petreczky, *Phys. Rev.*, **D91**(5), 054503 (2015), arXiv:1411.3018.
- [11] Yu Maezawa, Frithjof Karsch, Swagato Mukherjee, and Peter Petreczky, *PoS, LATTICE2015*, 199 (2016).
- [12] Bastian B. Brandt, Anthony Francis, Harvey B. Meyer, Owe Philipsen, Daniel Robaina, and Hartmut Wittig, *JHEP*, **12**, 158 (2016), arXiv:1608.06882.
- [13] Philipp Gubler, Teiji Kunihiro, and Su Houng Lee, *Phys. Lett.*, **B767**, 336–340 (2017), arXiv:1608.05141.
- [14] A. Bazavov et al., *Phys. Rev.*, **D86**, 034509 (2012), arXiv:1203.0784.
- [15] S. Ejiri, Y. Maezawa, N. Ukita, S. Aoki, T. Hatsuda, N. Ishii, K. Kanaya, and T. Umeda, *Phys. Rev.*, **D82**, 014508 (2010), arXiv:0909.2121.
- [16] Teiji Kunihiro, Shin Muroya, Atsushi Nakamura, Chiho Nonaka, Motoo Sekiguchi, and Hiroaki Wada, *Phys. Rev.*, **D70**, 034504 (2004), arXiv:hep-ph/0310312.